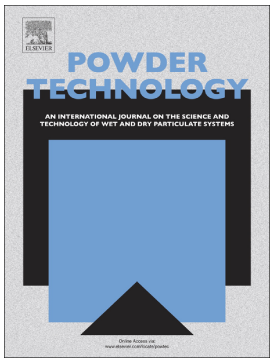

An investigation into the flowability of fine powders used in pharmaceutical industries

Vivek Garg, S.S. Mallick, Pablo-Garcia Trinanes, Robert James Berry

PII: S0032-5910(18)30444-3
DOI: doi:10.1016/j.powtec.2018.06.014
Reference: PTEC 13447

To appear in: *Powder Technology*

Received date: 7 August 2017
Revised date: 24 May 2018
Accepted date: 4 June 2018

Please cite this article as: Vivek Garg, S.S. Mallick, Pablo-Garcia Trinanes, Robert James Berry , An investigation into the flowability of fine powders used in pharmaceutical industries. Ptec (2017), doi:10.1016/j.powtec.2018.06.014

An investigation into the flowability of fine powders used in pharmaceutical industries

Vivek Garg[1*], S.S.Mallick[2], Pablo-Garcia Trinanes[1] and Robert James Berry[1]

[1]The Wolfson Centre for Bulk Solids Handling Technology, University of Greenwich, UK
[2]Department of Mechancial Engineering, Thapar University, India
*corresponding author: vg_guru768@yahoo.co.in

Abstract

This paper investigates into the flow properties of two popular pharmaceutical excipients (Calcium sulphate and Dicalcium phosphate) and their respective feeder hopper design requirements. There are numerous problems related to poor powder flowability that are faced by pharmaceutical industries, due to a lack of fundamental understanding of powder flow properties and their effects on hopper design parameters [1]. Characterization tests confirmed that the Dicalcium phosphate powder displayed a smaller particle size, larger specific surface area and higher value of Hausner ratio compared to Calcium sulphate powder indicating that Dicalcium phosphate powders are markedly more cohesive. This was validated by the instantaneous and time consolidation flow function curves which showed that the Dicalcium phosphate was the more cohesive. Powder flow function and wall friction tests were carried out on a ring type shear tester working on the basis of Jenike's principle. Based on the instantaneous test results, Dicalcium phosphate was found to require a larger hopper outlet dimension for the same hopper half angle compared to Calcium sulphate. The time consolidation test results have shown that both Dicalcium phosphate and Calcium sulphate gained strength during static storage and have become more cohesive. A simple empirical model for powder cohesion and unconfined yield stress has been developed and validated with a number of experimental values derived from common pharmaceutical powders.

Keywords: flow property testing, pharmaceutical excipients, flow function, time consolidation, hopper design

1. Introduction

In pharmaceutical industries, the active pharmaceutical ingredients and excipients combine together to form the final drug after passing through various intermediate processes, such as blending, transfer, storage, feeding, die filling, fluidization and encapsulation. There are various challenges currently being faced by pharmaceutical industries due to poor flowability of powders [2]. During the different processes which the powders pass through in the pharmaceutical industry, they undergo significant variation in their physical particle scale properties, which affect the bulk flow properties such the; flowability, bulk density, compaction, etc. Therefore, to maintain the efficiency of these processes, it is vital to monitor these variations. Apart from this, there could be a possibility of powder agglomeration, which would result in blockage, unstable discharge and subsequent stoppage of the equipment and processes. At the other extreme, excessively free flow, aeratable pharmaceutical powders could cause flooding during the filling operation, thus again compromising the process and product quality. Therefore, it is necessary to monitor the flowability variation at each processing step with close precision [3] and take appropriate measures to ensure that a desirable powder flow condition is maintained. To investigate the flowability of different powders, the classical procedure is to perform laboratory scale tests based on Jenike's principle. The method is based on the calculation of flow function curves under instantaneous and time consolidation stresses [4], as well as a wall friction locus and a bulk density (compressibility) curve. Other parameters, such as cohesion c, effective angle of internal friction δ_j and angle of internal friction φ, can be calculated by analyzing the Mohr's circle with the knowledge of major principal or consolidated stresses [5]. There are various powder characteristics, such as particle size distribution, particle shape, surface structure, particle

density, bulk density, water content and chemical composition on which the flowability of the powder depends. To characterize the flow properties of the powders, the shear cell technique is widely used [6] in designing storage bins and hoppers that are widely used in all kind of industrial processes, such as detergent, cement, food etc. [7-9]. However, it seems that there is a limited amount of information available in open literature on the flowability of powders used in pharmaceutical industries. The majority of the pharmaceutical drugs are blends of active and incipient are handled in a solid crystalline form. The challenge is controlling the flowability of the blend. If the material is too free flowing unwanted segregation of the blend components can occur, making them either ineffective or hazardous to human health. Conversely if the material is too cohesive then segregation is no longer a problem, but poor flow and unwanted adhesion problems may occur instead. To maintain the desired quality control on the drugs, it is essential to pre-determine the powder flowability and to investigate whether the powder contains the right mixture of all the required ingredients. Adequate powder flowability should be maintained for high speed tableting and encapsulation processes [10]. The use of glidants have become quite common for most of the pharmaceutical industries in order to reduce the issues of powder agglomeration and to maintain the powder flowability [11]. However, it has been reported that excess use of glidants may disturb the surface morphology and decrease the solubility properties of the drugs thus affecting the hardness range of the tablets [12]. Hence, to maintain better flowability of the powders without the use of glidants, it is essential to design the storage facilities correctly which requires thorough investigation on the powder flowability. Powder flowability characteristics can undergo significant unitended changes in storage, e.g. long storage period could result in compacted bulk powders, which would subsequently reduce the powder flowability due to the gain in strength. This could be caused by a possible changes in the

physico-chemical interaction at inter-particle contacts and through exposure to changes in environmental conditions (i.e. temperature, relative humidity) [13]. A limited amount of literature is available covering the comparison between instantaneous and time consolidated flow characteristics [14, 15]. Studies on the time consolidation effect on the powder behavior have been carried out mainly for food powders [16], but such information is generally missing for pharmaceutical powders [17]. The objective of this paper is to investigate into the flow properties of Calcium sulphate and Dicalcium phosphate powders subjected to instantaneous and time consolidation conditions and to use such information to effectively design industrial storage systems. The aim is to provide the industry a reliable design guidelines to enable the powders to flow adequately under the influence of gravity, without the requirement of artificially improving the flowability of the powders that may compromise the medicinal effectiveness of the drugs. The literature reports that during consolidation and under the influence of inter-particle adhesive forces, cohesive arches are formed. Usually, two types of flow patterns of powders are prevalent in storage hoppers: mass and funnel flow. The more desirable mode is the mass flow, because in this type of flow, all the particles flow simultaneously in a first-in, first out basis, thus assisting in achieving better product and process quality control. Powders such as Calcium sulphate and Dicalcium phosphate are widely used in pharmaceutical industries as excipients, hence these products have been selected as case study materials in this paper.

2. Materials and methods

2.1 Characterization of powders

In the present study, samples of Calcium sulphate and Dicalcium phosphate powders were obtained from VIP Pharmaceuticals Pvt. Ltd. Each sample was preheated in a baking oven at 103°C for 3 hours for the purpose of removing any moisture content as per ASTM D 2974-87. A chemical characterization of the samples was undertaken using Energy-dispersive X-ray spectroscopy. In the Calcium sulphate powder sample, calcium, sulphur and oxygen contents were found to be 19.35, 17.44 and 63.21% by weight, respectively. With respect to the Dicalcium phosphate powder sample, the weight percentage of calcium, phosphate and oxygen were 41.29, 12.72 and 45.99%, respectively.

Particle size distribution and specific surface area

Particle size distribution and specific surface area (SSA) of the Calcium sulphate and Dicalcium phosphate powders were determined by laser light scattering using a Malvern Mastersizer 3000 (Malvern Instruments, Worcestershire, UK) instrument. Span values were determined using equation 1 to evaluate the particle size distribution.

$$Span = (d_{90} - d_{10})/d_{50} \quad (1)$$

where, d_{50} represents the diameter below which half of the powder population lies, while 10 and 90% of the distribution lies below the size values of d_{10} and d_{90}, respectively.

Bulk and particle densities

The bulk density of a powder is defined as the mass of powder divided by the volume occupied. The bulk density of a powder can undergo considerable changes depending on the different processes through which the bulk powder passes, such as packing, compaction, consolidation, fluidization etc. Loose poured bulk density represents the random loose packing of a powder and its value is measured by allowing mildly aerated powder to settle in a container under the influence of gravity (without the application of any other external loading) [18]. A powder with a strong structural strength (i.e. strong particle-particle-wall bonding) will exhibit a low bulk density, as it will tend to resist collapsing when dispersed in a container. Furthermore, high friction between the particles will resist rearrangement of the powders towards achieving high packing fraction, thus contributing to low bulk density. Conversely, a structurally weak powder will exhibit a high bulk density, as it will collapse readily when left to settle, especially under tapping. Also, low friction between the particles will facilitate in easier rearrangement of the particles more easily, which in turn would result in a higher; packing fraction and bulk density [19]. Porosity [20,21] and compressibility index [22] were determined using the following formulae:

$$Porosity = 1 - (\rho_{lb} - \rho_p) \quad (2)$$

$$Compressibity\ Index = 100 \times [1 - \rho_{lb}/\rho_t] \quad (3)$$

The particle density (ρ_p) of samples was determined using a water displacement method. The ratio of the tapped to loose poured bulk density is defined as the Hausner ratio, which is a useful measure of cohesion and particle to particle friction [19]. A drop in the value of Hausner ratio represents decrease in cohesiveness of the powders.

Scanning Electron Microscopy

Scanning Electron Microscope (SEM) images were captured at the Sophisticated Analytical Instruments Laboratory of Thapar University, Patiala. The powders were placed on Aluminium stubs using double-sided carbon tape and coated with a 5-mm layer of gold/palladium (Au: Pd ¼ 80:20) in JSM-5510 Scanning Electron Microscope (make: JEOL Ltd). The instrument was operated at an accelerating voltage of 15 kV and the images were taken at a magnification of 1000x.

2.2 Powder flow property testing

The Powder Flow Tester (PFT) of Brookfield Engineering Laboratories, Inc., Middleboro, MA, USA was used to experimentally determine the flow properties of Calcium sulphate and Dicalcium phosphate at the Laboratory for Particle and Bulk Solid Technologies, Thapar University. The Powder Flow Tester (PFT) works on the principles of Jenike's methodology. It has an annular shear cell, in which the sample is filled and the consolidation stress is applied to

the powder through an annular lid. The axial and torsional speeds for the PFT were 1.0 mm/s and 1 rev/hr., respectively. These were applied to produce shear in the sample under a given consolidation stress. Samples were filled into the Aluminium trough of the annular shear cell at room temperature (22 to 25°C). The powder surface in the trough for flow- or wall-fiction tests were levelled using curved- or flat-profiled shaping blades, respectively. Of the two available lids, the flow function lid was used to measure yield locus in the powder and wall friction tests were conducted with standard wall friction lid made of 304 stainless steel with 2B surface finish. Vane or flat profiled lids were attached to the compression plate for flow or wall friction tests. The equipment was automated with the Powder Flow Pro software for analylys of the raw data and providing yield locus, flow function curves, trends for wall friction angle versus normal stress, angle of internal friction as a function of major principle consolidating stress, time consolidation information and hopper half angle. For the standard flow function tests, the applied uniaxial normal stresses were in the range between 0.2 and 4.8 kPa. Ten normal stresses were applied between 0.4 and 4.8 kPa to measure the wall friction angles for the standard wall friction tests.

3. Results and discussions

3.1 Physical properties of powders

Table 1 provides the various physical properties of Calcium sulphate and Dicalcium phosphate powders. Table 1 shows that the average particle size of Dicalcium phosphate powders is less than that of Calcium sulphate powders. This indicates the presence of more fines in Dicalcium

phosphate. As a result, the specific surface area is more for Dicalcium phosphate powders (as shown in Table 1). Smaller particle size and the presence of more fines in case of Dicalcium phosphate would cause larger amounts of Van der Waals forces of attraction (adhesion) amongst the particles [6]. Additionally, larger specific surface area of dicalcium phosphate powders would cause greater surface resistance [23]. The Hausner ratio value of Dicalcium phosphate is larger than Calcium sulphate. This indicates that the Dicalcium phosphate powders can be compressed to relatively larger tapped density than Calcium sulphate powders. This further points out that the Dicalcium phosphate powders have stronger particle-particle cohesion and as a result, it would exhibit poor flowability compared to the Calcium sulphate powders. The contributing factor for achieving relatively larger tapped density for Dicalcium phosphate is that the Dicalcium phosphate powders were having larger particle to particle air gaps (greater amount of porosity) under the loose poured condition [24]. Therefore, when tapped, the dicalcium phosphate powders could occupy those void spaces more readily than the Calcium sulphate powders, which having less void spaces under the loose poured condition. As a result, the Calcium sulphate powder had lesser amount of void spaces for the fines to occupy under the application of tapping. The results of particle size, surface area, Hausner ratio and porosity all indicate that the Dicalcium phosphate powders are likely to be a poorer flowable powder compared to Calcium sulphate powders.

Table 1: Physical properties of Calcium sulphate and Dicalcium phosphate

Figure 1 shows the Scanning Electron Microscopy (SEM) images of Calcium sulphate and Dicalcium phosphate powders. The morphology of the Calcium sulphate particles is dominated by acicular particles with sharp edges. The cohesive nature of the dicalcium phosphate powder

is clearly shown in Fig. 1.b demonstrated by the formation of agglomerates of multiple indivicual particles.

(a) Calcium sulphate Sample (b) Dicalcium Phosphate Sample

Figure 1: SEM images of Calcium sulphate and Dicalcium phosphate samples

3.2 Flow properties of Calcium sulphate and Dicalcium phosphate powders

Yield locus and flow function curves

The yield locus of a powder represents the shear stress (τ) necessary to initiate the flow in the powder sample under a given consolidation stress (σ) [25] which in it's simplest form can be represented by the Mohr–Coulomb failure criteria (equation 4) at any given pre-shear condition.

$$\tau = \sigma \tan \varphi + C \quad (4)$$

Where, φ is the internal friction angle representing the magnitude of friction between the layers of powder. The values of pre-shear stresses for Calcium sulphate were 0.310, 0.608, 1.205, 2.410 and 4.847 kPa, whereas the same for dicalcium phosphate powders were 0.316, 0.614, 1.214, 2.421 and 4.859 kPa, respectively (Figure-2). Each yield locus provides major consolidation stress (σ_1) and the corresponding values of unconfined yield strength (σ_c) related to

the powder. The stress range represents the operation range of the Brookfield PFT and is appropriate to the stress levels occurring in small volume pharmaceutical feed hoppers.

Figure 2: Example of Yield loci and main Mohr circles for Calcium sulphate obtained by applying 4.847 kPa.

Figure 3 shows the flow function curve (a plot between σ_1 and σ_c) for Dicalcium phosphate and Calcium sulphate. The flow function curve (Figure 3) has been divided in four parts based on Jenike's flowability classification [24], as reported by [26]. The Flow Index (FI) is the reciprocal of flow function curve slope (σ_1/σ_c) and indicates the relative flowability of the powders. Typical values of Flow Index (FI) and the slope of flow function curve for Calcium sulphate at a pre-shear value of 1.2 kPa were 3.802 and 0.13, respectively. Values of the same parameters under the same pre-shear condition for Dicalcium phosphate were 1.933 and 0.32, respectively. Figure 3 shows that below the major principal consolidation stress of about 2.5 kPa, the Dicalcium phosphate powders fell in the "cohesive" regime. However, above this consolidation stress, this powder fell into the "easy flowing" regime. By contrast the Calcium sulphate powders remained in the "easy flowing" regime up to a consolidation stress of 3.2 kPa and beyond this stress, it entered into the "free flowing" range. The reason for Dicalcium phosphate being more cohesive compared to Calcium sulphate powder has been already explained in the previous section. Figure 3 is based on instantaneous flow function results.

Figure 3: Flow function curves for Calcium sulphate and Dicalcium phosphate based on instantaneous flow function test results

Effective angle of internal friction (δ) is the ratio of major consolidation and minor consolidation stresses over the powder element in steady state flow [27]. The trend of variation of effective angle of internal friction with major consolidation stress is given in Figure 4.

Figure 4: Effective angle of internal friction versus major consolidation stress for Dicalcium phosphate and Calcium sulphate

The effective angle of internal friction of powders represents the relative contribution of adhesive forces to frictional forces. Figure 4 shows that the effective angle of internal friction values are larger at lower consolidation stresses for both the powders. The increment is considerably larger for Dicalcium phosphate indicating that this powder is more cohesive than Calcium sulphate. The reason for the Dicalcium phosphate powders having higher values of effective angle of internal friction is that the dicalcium phosphate powders were having larger adhesive forces than Calcium sulphate (due to the smaller particle size, larger specific surface area, irregular structure of dicalcium phosphate powders etc. compared to Calcium sulphate, as explained in the previous section) and also as represented by Figure 3. The reason for the decreasing nature of the slopes with increasing values of major consolidation stress is that although both the forces of particle to particle friction and adhesion increase simultaneously (as

consolidation causes the particles to come closer to each other) with the increase of major consolidation stress, but the increase of frictional forces between the particles caused due to enhanced surface to surface contact friction and interlocking is far greater than the increase in adhesive forces, such as the Van der Waals effect [24]. As a result of larger prevalence of frictional forces at larger values of major principal consolidation stresses, the effective angle of internal friction decreases at higher major consolidation stresses. Table 2 provides different states of stress conditions with some typical values of instantaneous flow property testing.

Table 2: Sample test data for flow property testing for Calcium sulphate and Dicalcium phosphate

Wall friction and bulk density tests

Figure 5 shows the trends of wall friction angles versus normal stress for Dicalcium phosphate and Calcium sulphate powders. The friction between wall material and the powder layer adjacent to the walls at a given normal stress is given by wall friction angle (φ_w).

Figure 5: Trends of wall friction angle versus major consolidation stress for Dicalcium phosphate and Calcium sulphate powders

It can be seen from Figure 5 that the wall friction angle decreases with an increase in normal stress. The Dicalcium phosphate powders were having smaller particle diameter and larger specific surface area compared to Calcium sulphate powders. This would cause higher adhesion and surface friction for the case of Dicalcium phosphate due to more particle surface to wall contact. Figure 6 shows the variation of bulk density with an increase in normal stress for dicalcium phosphate and Calcium sulphate powders. The trends of bulk density versus normal stress for both the powders follow a relatively sharper rising curve at low normal stress values. After the initial sharp rise, the curves tend to get flatten out in the higher stress value ranges.

Figure 6: Bulk density versus normal stress for Dicalcium phosphate and Calcium sulphate powders

Time consolidation tests

Certain bulk powders gain additional strength when stored at rest under compressive stress for a long-time period. This effect is known as time consolidation [24]. This may happen when the

powders are stored overnight or over the weekend or during the shutdown condition in a plant, e.g. pharmaceutical industry. Gains in strength due to time consolidation is caused by visco-plastic or plastic deformation at particle contact zones resulting in the enhancement of adhesive forces due to the shortening of distance between the particles and increase in contact areas, development of solid bridges due to solid crystallization during the drying of moist bulk solids etc. [24]. In time consolidation tests, the sample was subjected to a static load (i.e. it was not sheared) for a time span is 12 hours. This time frame was selected as representative of the overnight storage period used for these powders(Calcium sulphate and Dicalcium phosphate). Table 3 and 4 compare the unconfined yield stress for Calcium sulphate and dicalcium phosphate powders before and after time consolidation under different pre-shear stress applications.

Table 3: Unconfined yield strength for Calcium sulphate before and after time consolidation

Table 4: Unconfined yield strength for Dicalcium phosphate before and after time consolidation

A comparison of unconfined yield strength results before and after time consolidation (Table 3 and 4 show) that both the powders gained additional strength after time consolidation. Figure 7 presents flow function curves for Calcium sulphate and Dicalcium phosphate after time consolidation. Figure 7 reveals that the Calcium sulphate powders have become "cohesive" at low stresses after time consolidation from being "easy flowing" before time consolidation; the Dicalcium phosphate powders have continued to remain in "cohesive" zone (but with a greater portion inside the "cohesive regime compared to the instantaneous flow function results).

Figure 7: Flow function curves for Dicalcium phosphate and Calcium sulphate powders based on time consolidation test results

Critical dimensions of mass flow hopper

The conical hopper half angle (θ) and outlet diameter (D) are the critical parameters for hopper design especially to maintain reliable mass flow of powders. Jenike, A.W., 1964, carried out pioneering work by deriving mathematical relations powder flow properties. Hopper half angles and critical outlet openings were determined from equations (5) and (6) by using the results obtained from flow property and wall friction tests (corresponding to instantaneous and time consolidation tests). The critical mass flow geometries for reliable gravity flow are likely to be incompatible with the instantaneous mass flow rates that are required for processing the material. I.e. the outlet sizes for gravity flow is much larger than the outlet size required to give the required feed rate (grams/second). Therefore the material would be processed through an agitated screw feeder, where powder is continuously stirred to keep it flowing and enable it to pass through an outlet that is an order of magnitude smaller than the minimum critical outlet size. However, while the measurements may not be useful in the context of silo design, they provide a useful measure of flowability, that can be used to assist in the optimization of the flow properties of the blend. What is required for blend optimization is a balance between a free flow powder which will create to unwant segregation of the blend components and an excessively cohesion powder which will overcome the agitated feeder. The results are shown in Figure 8.

$$D = \frac{2\ X\ \sigma_c\ X\ 1000}{\rho_b\ X\ g} \tag{5}$$

$$\theta = \left[90 - \frac{1}{2}\cos^{-1}\left(\frac{1-\sin\delta}{2\sin\delta}\right)\right] - \frac{1}{2}\left[\varphi_w + \sin^{-1}\left(\frac{\sin\varphi_w}{\sin\delta}\right)\right] \tag{6}$$

Figure 8: Comparison of hopper half angle to outlet dimension for Calcium sulphate and Dicalcium phosphate powders with and without time consolidation effects

Figure 8 shows that the Dicalcium phosphate powder would require wider hopper outlet dimensions compared to the Calcium sulphate powders. This is due to the larger cohesion in case of Dicalcium phosphate powders as shown in Figure 9.

Figure 9: Cohesion versus Consolidation for Dicalcium phosphate and Calcium sulphate powders

Also, it is found that time consolidation has a stronger effect on Calcium sulphate. For this powder, a considerable amount of additional hopper outlet size is required (for the same hopper angle) after time consolidation compared to the requirement outlet openings obtained from instantaneous test results. The results indicate that 12 hrs. of consolidation time is inadequate to result in any considerable difference in the flow behavior (or design of hopper dimensions) for Dicalcium phosphate powders.

Modelling for Cohesion and Unconfined yield stress

A new simple empirical model has been developed to study the effect of physical properties on cohesion and unconfined yield strength. The values of cohesion and unconfined yield stress

within five pre-shear stresses can be obtained. In the model, cohesion has been taken as a function of adequate particle size, compressibility index and pre-shear stress. Selective determination of correlation coefficients shows that CI and σ_{pre} have higher influence on cohesion and unconfined yield stress than the effective particle size. The cohesion model is given by: -

$$C = 0.00125\ (d_{50}/S)^{0.092}(CI)^{1.665}\left(\sigma_{pre}\right)^{0.652} \qquad [r^2 = 0.925]$$

The Unconfined yield stress model is given by: -

$$\sigma_c = 0.01409(d_{50}/S)^{0.091}(CI)^{1.277}\left(\sigma_{pre}\right)^{0.707} \qquad [r^2 = 0.93]$$

The comparison of the modeled cohesion values and the cohesion values obtained experimentally are demonstrated in Figure 10 by adding common pharmaceutical powders in the less than 100 microns size range. More details can be found from Table.5.

Table 5: Properties of different materials used for modelling.

Figure 10: Comparison between experimental cohesion and modelled cohesion at all σ_{pre}

The above figure shows that after performing regression analysis, there is 92% similarity in the values that were obtained through the model and the experimental data from the powder flow tester. The comparison of modeled σ_c values versus experimental σ_c values are demonstrated in Figure 11.

Figure 11. Comparison between experimental unconfined yield stress and modelled unconfined yield stress at all σ_{pre}

4. Conclusions

Physico-chemical characteristics and the flow properties of two widely used pharmaceutical excipients, namely Calcium sulphate and dicalcium phosphate, were studied with and without time consolidation effects. The Dicalcium phosphate powders were found to be more cohesive than the Calcium sulphate powders as indicated by larger porosity and larger tapped density of the Dicalcium phosphate powders and corroborated by the powder mechanics analysis thus requiring wider hopper outlet dimensions than the Calcium sulphate powders in abscense of time consolidation. Time consolidation has been found to have a stronger effect on Calcium sulphate, requiring a considerably a larger hopper outlet dimension (for the same hopper angle) after time

consolidation. The results clearly indicate that a reliable hopper design should be based on specific powder property data. The hopper that may allow Calcium sulphate to flow easily (maintaining mass flow condition) may not be adequate for Dicalcium phosphate. Time consolidation test plays a major role in designing storage facilities of powders that are stored overnight. These powders may suffer alterations on their flow properties over time and could potentially result in severe flow problems (such as arching). A mathematical model has also been developed for determining the value of cohesion and unconfined yield stress. For a good design, the engineer is recommended to carry out necessary flow property testing with and without time consolidation effects into consideration for designing practical storage or feeding systems to achieve desirable mass flow condition.

Nomenclature

C	Cohesion, kPa
D	Minimum opening size, mm
mg	Particle weight, N
d	Particle size diameter, μm
θ	Hopper half angle, °
σ	consolidation stress or normal stress, kPa
σ_{pre}	Pre-shear stress, kPa
τ	Shear stress, kPa
σ_1	Major principle stress, kPa
σ_c	Unconfined yield strength, kPa
φ	Angle of internal friction, °
ρ_{lb}	Loose poured bulk density, Kg/m^3
ρ_p	Particle density, Kg/m^3
ρ_t	Tapped bulk density, Kg/m^3
φ_w	Wall friction angle, °
$\sigma_{c,\ min}$	Minimum unconfined yield strength, kPa
δ	Effective angle of internal friction, in degrees

Abbreviations

FI	Flow Index
RH	Relative Humidity

PFT	Powder Flow Tester
SEM	Scanning Electron Microscopy
SSA	Specific Surface Area

References

[1] Standard, A.S.T.M., 2008. D6773: Standard shear test method for bulk solids using the Schulze ring shear tester. *ASTM International.*

[2] Ripp, M., Debele, Z.A. and Ripperger, S., 2015. Determination of Bulk Flow Property of tef Flour and Seed and Design of a Silo. *Particulate Science and Technology*, *33*(5), pp.494-502.

[3] Koynov, S., Glasser, B. and Muzzio, F., 2015. Comparison of three rotational shear cell testers: Powder flowability and bulk density. *Powder Technology, 283*, pp.103-112.

[4] Bian, Q., Sittipod, S., Garg, A. and Ambrose, R.K., 2015. Bulk flow properties of hard and soft wheat flours. *Journal of Cereal Science*, *63*, pp.88-94.

[5] Leung, L.Y., Mao, C., Chen, L.P. and Yang, C.Y., 2016. Precision of pharmaceutical powder flow measurement using ring shear tester: High variability is inherent to powders with low cohesion. *Powder Technology*, *301*, pp.920-926.

[6] Amagliani, L., O'Regan, J., Kelly, A.L. and O'Mahony, J.A., 2016. Physical and flow properties of rice protein powders. *Journal of Food Engineering*, *190*, pp.1-9.

[7] Opaliński, I., Chutkowski, M. and Hassanpour, A., 2016. Rheology of moist food powders as affected by moisture content. *Powder Technology*, *294*, pp.315-322.

[8] Freeman, R., 2007. Measuring the flow properties of consolidated, conditioned and aerated powders—a comparative study using a powder rheometer and a rotational shear cell. *Powder Technology*, *174*(1), pp.25-33.

[9] Fitzpatrick, J.J., Barringer, S.A. and Iqbal, T., 2004. Flow property measurement of food powders and sensitivity of Jenike's hopper design methodology to the measured values. *Journal of Food Engineering*, *61*(3), pp.399-405.

[10] Dudhat, S.M., Kettler, C.N. and Dave, R.H., 2016. To Study Capping or Lamination Tendency of Tablets Through Evaluation of Powder Rheological Properties and Tablet Mechanical Properties of Directly Compressible Blends. *AAPS PharmSciTech*, pp.1-13.

[11] Trementozzi, A.N., Leung, C.Y., Osei-Yeboah, F., Irdam, E., Lin, Y., MacPhee, J.M., Boulas, P., Karki, S.B. and Zawaneh, P.N., 2017. Engineered particles demonstrate improved flow properties at elevated drug loadings for direct compression manufacturing. *International journal of pharmaceutics*, *523*(1), pp.133-141.

[12] Morin, G. and Briens, L., 2013. The effect of lubricants on powder flowability for pharmaceutical application. *AAPS PharmSciTech*, *14*(3), pp.1158-1168.

[13] Sun, C.C., 2016. Quantifying effects of moisture content on flow properties of microcrystalline cellulose using a ring shear tester. *Powder Technology*, *289*, pp.104-108.

[14] Wang, Y., Koynov, S., Glasser, B.J. and Muzzio, F.J., 2016. A method to analyze shear cell data of powders measured under different initial consolidation stresses. *Powder Technology*, *294*, pp.105-112.

[15] Jan, S., Jan, K. and Saxena, D.C., 2016, January. Flow property measurement of rice flour-A Review. In *MATEC Web of Conferences* (Vol. 57). EDP Sciences.

[16] Slettengren, K., Xanthakis, E., Ahrné, L. and Windhab, E.J., 2016. Flow Properties of Spices Measured with Powder Flow Tester and Ring Shear Tester-XS. *International Journal of Food Properties*, *19*(7), pp.1475-1482.

[17] Wang, Y., Snee, R.D., Meng, W. and Muzzio, F.J., 2016. Predicting flow behavior of pharmaceutical blends using shear cell methodology: A quality by design approach. *Powder Technology*, *294*, pp.22-29.

[18] Jaggi, V., Leaper, M.C. and Ingham, A., 2016. Measuring the flow properties of small powder samples using an avalanche tester. *Drying Technology*, *34*(6), pp.723-728.

[19] Abdullah, E.C. and Geldart, D., 1999. The use of bulk density measurements as flowability indicators. *Powder Technology*, *102*(2), pp.151-165.

[20] Li, R., Roos, Y.H. and Miao, S., 2016. Influence of pre-crystallisation and water plasticization on flow properties of lactose/WPI solids systems. *Powder Technology*, *294*, pp.365-372.

[21] Li, R., Roos, Y.H. and Miao, S., 2016. The effect of water plasticization and lactose content on flow properties of dairy model solids. *Journal of Food Engineering*, *170*, pp.50-57.

[22] Ji, J., Fitzpatrick, J., Cronin, K., Fenelon, M.A. and Miao, S., 2017. The effects of fluidised bed and high shear mixer granulation processes on water adsorption and flow properties of milk protein isolate powder. *Journal of Food Engineering*, *192*, pp.19-27.

[23] Anjaneyulu, P. and Khakhar, D.V., 1995. Rheology of a gas-fluidized bed. *Powder technology*, *83*(1), pp.29-34.

[24] Schulze, D., 2008. Powders and bulk solids. *Behaviour, Characterization, Storage and Flow. Springer*.

[25] Jager, P.D., Bramante, T. and Luner, P.E., 2015. Assessment of Pharmaceutical Powder Flowability using Shear Cell- Based Methods and Application of Jenike's Methodology. *Journal of pharmaceutical sciences*, *104*(11), pp.3804-3813.

[26] Saw, H.Y., Davies, C.E., Paterson, A.H. and Jones, J.R., 2015. Correlation between powder flow properties measured by shear testing and Hausner ratio. *Procedia Engineering*, *102*, pp.218-225.

[27] Jenike, A.W., 1964. Storage and flow of solids, bulletin no. 123. *Bulletin of the University of Utah, 53*(26).

Table 1: Physical properties of Calcium sulphate and Dicalcium phosphate

Powders	**d_{10} (µm)**	**d_{50} (µm)**	**d_{90} (µm)**	**Span**	**ρ_{lb} (kg/m^3)**	**ρ_p (kg/m^3)**	**ρ_t (kg/m^3)**	**Hausner Ratio (HR)**	**CI**	**Porosity**	**SSA (m^2/kg)**
Calcium sulphate	9	47	73	1.361	776	2500	921	1.186	15.75	0.689	152
Dicalcium phosphate	7	23	64	2.478	964	3333	1316	1.365	26.75	0.711	225

Table 2: Sample test data for flow property testing for Calcium sulphate and Dicalcium phosphate

Consolidation endpoint (kPa)	**Major principal consolidating stress (kPa)**	**Unconfined failure strength (kPa)**	**Angle (°)**	**Cohesion (kPa)**	**Effective angle of internal friction (°)**
Calcium sulphate					
0.31	0.696	0.336	33.8	0.09	48
0.608	1.387	0.478	36.3	0.121	45.4
1.205	2.8	0.735	37.1	0.183	43.7
2.41	5.692	1.147	38	0.28	42.9
4.847	11.68	1.817	38.6	0.437	42.3
Dicalcium phosphate					
0.316	0.589	0.47	22.1	0.158	56.3
0.614	1.147	0.725	25	0.231	47.8
1.214	2.314	1.197	27.9	0.361	44.6
2.421	4.63	2.033	30	0.587	43.2
4.859	9.399	3.347	31.7	0.933	41.8

Table 3: Unconfined yield strength for Calcium sulphate before and after time consolidation

Sample	**σ_c at σ_{pre1} kPa**	**σ_c at σ_{pre2} kPa**	**σ_c at σ_{pre3} kPa**	**σ_c at σ_{pre4} kPa**
Calcium sulphate (before time consolidation test)	0.336	0.478	0.735	1.147
Calcium sulphate (after time consolidation test-1)	0.498	0.684	0.932	1.398
Calcium sulphate (after time consolidation test-2)	0.527	0.894	0.989	1.624
Calcium sulphate (after time consolidation test-3)	0.576	0.897	1.158	1.697
Calcium sulphate (after time consolidation test-4)	0.597	0.901	1.274	1.924

Table 4: Unconfined yield strength for Dicalcium phosphate before and after time consolidation

Sample	**σ_c at σ_{pre1} kPa**	**σ_c at σ_{pre2} kPa**	**σ_c at σ_{pre3} kPa**	**σ_c at σ_{pre4} kPa**
Dicalcium phosphate (before time consolidation test)	0.462	0.738	1.224	2.027
Dicalcium phosphate (after time consolidation test-1)	0.544	0.863`	1.281	1.933
Dicalcium phosphate (after time consolidation test-2)	0.594	1.231	1.361	2.015
Dicalcium phosphate (after time consolidation test-3)	0.662	1.587	1.403	2.071
Dicalcium phosphate (after time consolidation test-4)	0.715	1.674	1.420	2.064

Table 5: Properties of different materials used for modelling.

S.No.	Sample	d_{50} (µm)	Span	CI	σ_{pre} (kPa)	Experimental (kPa)	Modelled C (kPa)	Experimental σ_c (kPa)	Modelled σ_c (kPa)
1.	Magnesium Tri-Silicate	33	1.424	24.91	0.301	0.16	0.1612	0.458	0.486
					0.597	0.225	0.2518	0.712	0.789
					1.194	0.329	0.3956	1.118	1.288
					2.404	0.516	0.6234	1.823	2.111
					4.839	0.871	0.9841	3.177	3.466
2.	Paracetamol	22	2.54	26.41	0.3	0.179	0.1619	0.596	0.478
					0.596	0.323	0.2532	1.016	0.777
					1.195	0.574	0.3984	1.829	1.270

					2.402	0.913	0.6279	2.97	2.082
					4.839	1.441	0.9911	4.713	3.417
3.	Lactose	64	2.31	21.21	0.306	0.156	0.1267	0.525	0.407
					0.603	0.233	0.1972	0.904	0.658
					1.201	0.354	0.3089	1.555	1.071
					2.407	0.595	0.4860	2.754	1.751
					4.843	1.019	0.7664	4.763	2.872
4.	Starch	41	1.809	23.63	0.303	0.111	0.1391	0.309	0.428
					0.600	0.178	0.2171	0.522	0.695
					1.19	0.285	0.3405	0.874	1.133

					7				
					2.404	0.399	0.5364	1.352	1.856
					4.839	0.674	0.8462	2.364	3.045

Highlights

- Flow properties of calcium sulphate and di-calcium phosphate powders were studied
- Annular shear tester following Jenike principle was used
- Di-calcium phosphate powder was found to be more cohesive than calcium sulphate
- Di-calcium phosphate requires larger hopper outlet compared to calcium sulphate
- Di-calcium phosphate changes flow property considerably under time consolidation

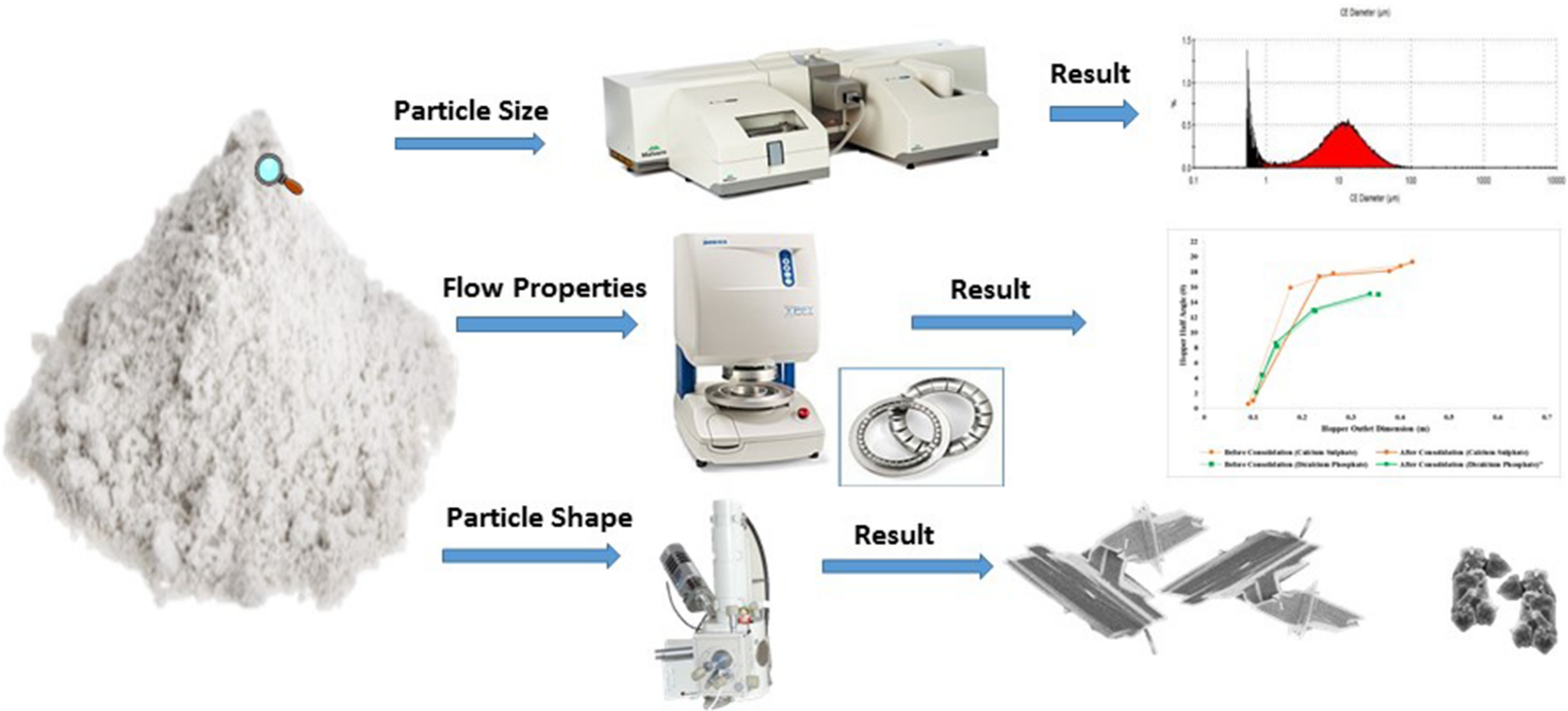

Graphics Abstract

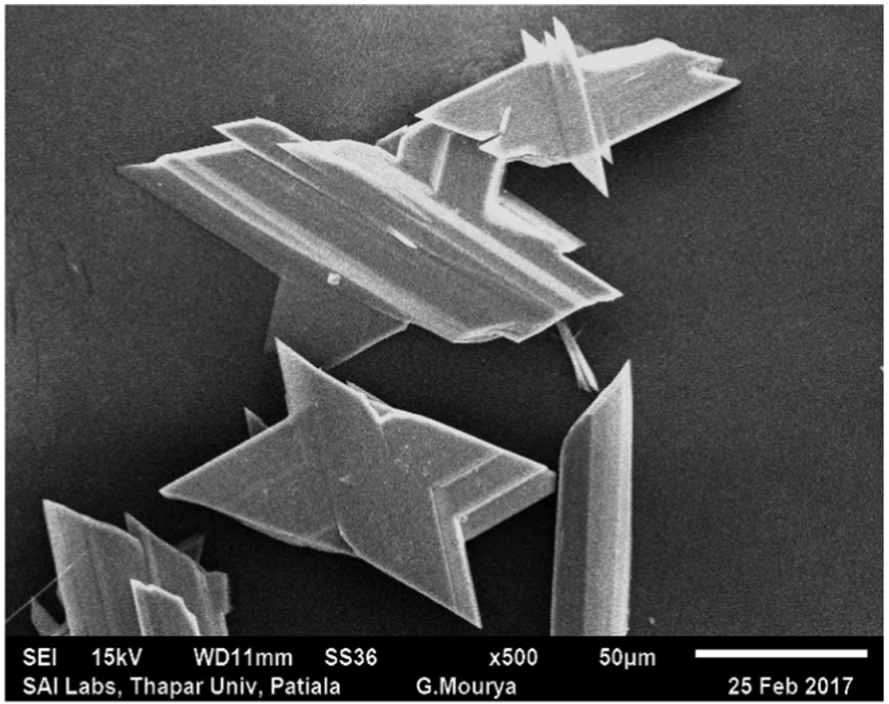
SEI 15kV WD11mm SS36 x500 50µm
SAI Labs, Thapar Univ, Patiala G.Mourya 25 Feb 2017

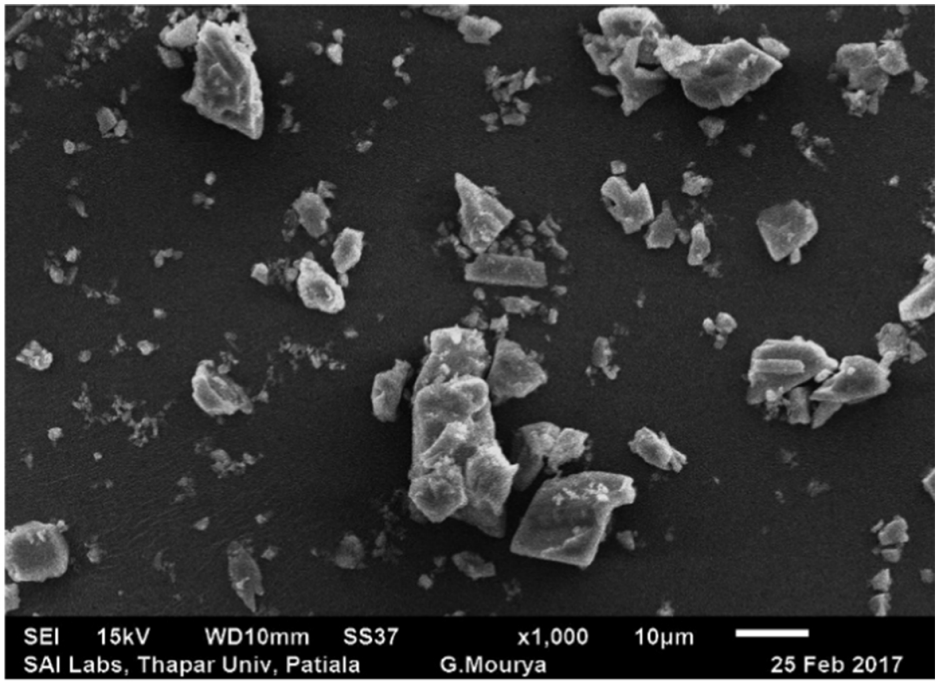
SEI 15kV WD10mm SS37 x1,000 10µm
SAI Labs, Thapar Univ, Patiala G.Mourya 25 Feb 2017

Figure 1

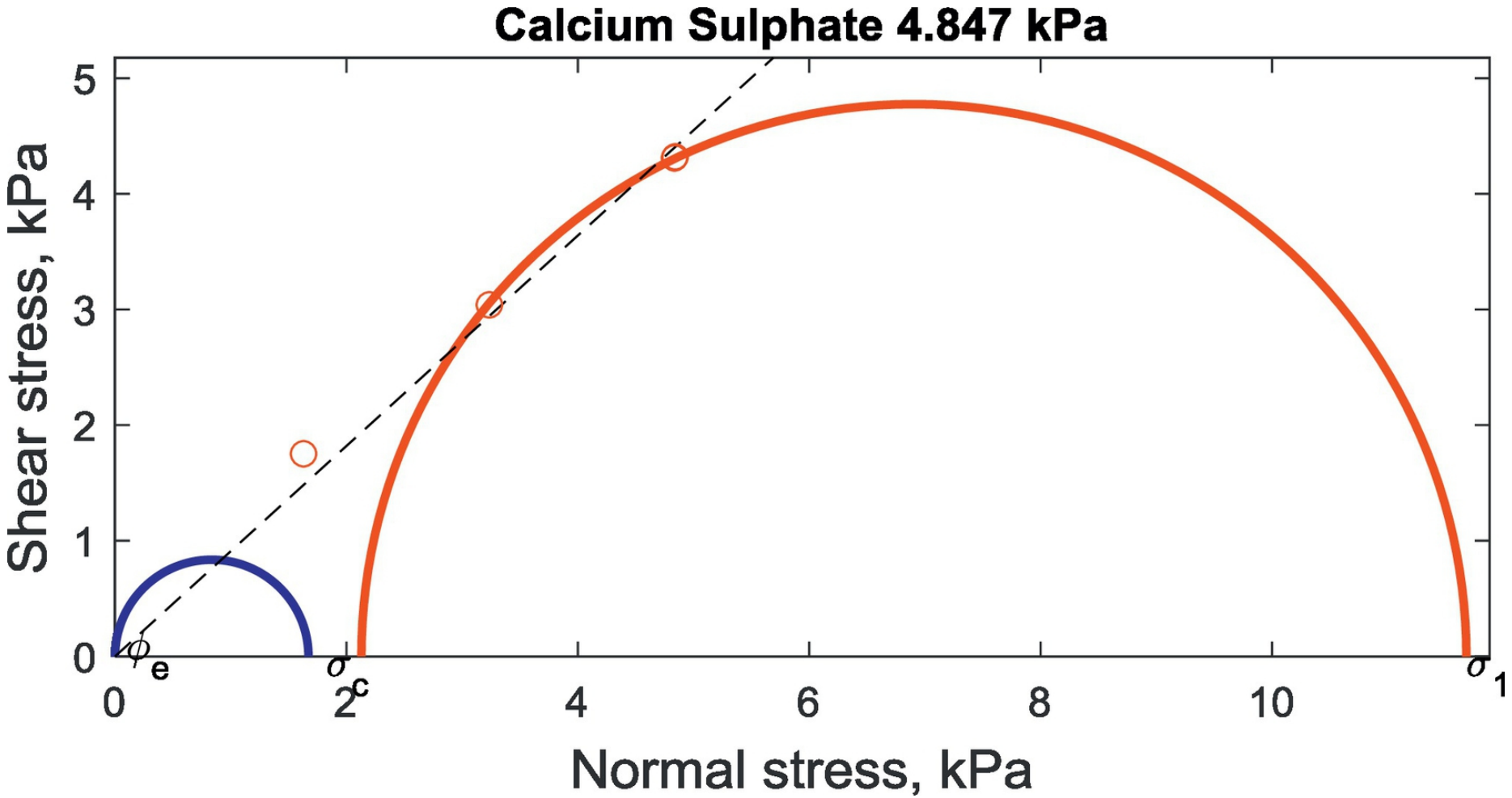
Calcium Sulphate 4.847 kPa
Shear stress, kPa
Normal stress, kPa
0
1
2
3
4
5
0
2
4
6
8
10
ϕ_e
σ_c
σ_1

Figure 2

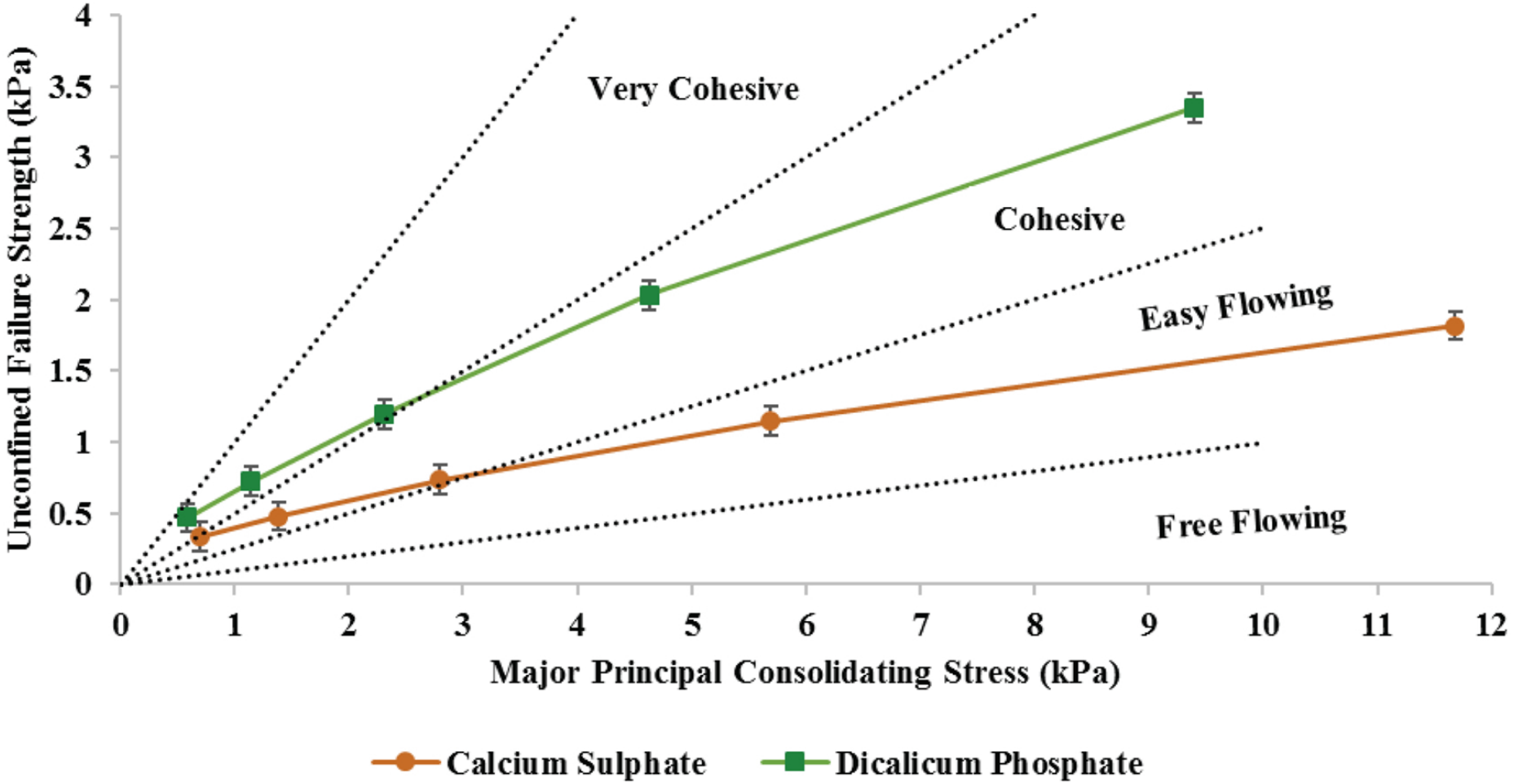
Unconfined Failure Strength (kPa)
4
3.5
3
2.5
2
1.5
1
0.5
0
Very Cohesive
Cohesive
Easy Flowing
Free Flowing
0
1
2
3
4
5
6
7
8
9
10
11
12
Major Principal Consolidating Stress (kPa)
Calcium Sulphate
Dicalicum Phosphate

Figure 3

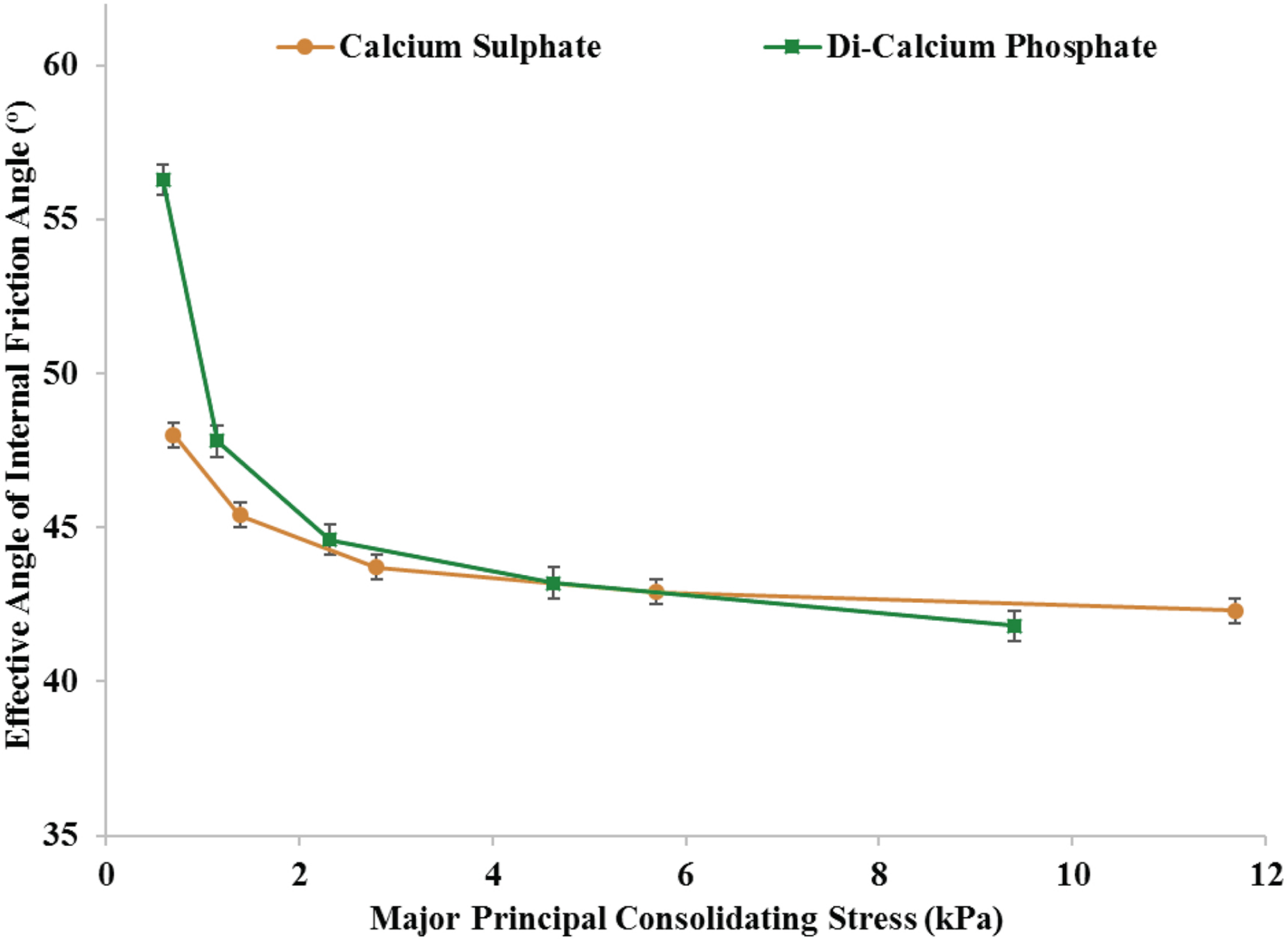
Calcium Sulphate
Di-Calcium Phosphate
Effective Angle of Internal Friction Angle (°)
60
55
50
45
40
35
0
2
4
6
8
10
12
Major Principal Consolidating Stress (kPa)

Figure 4

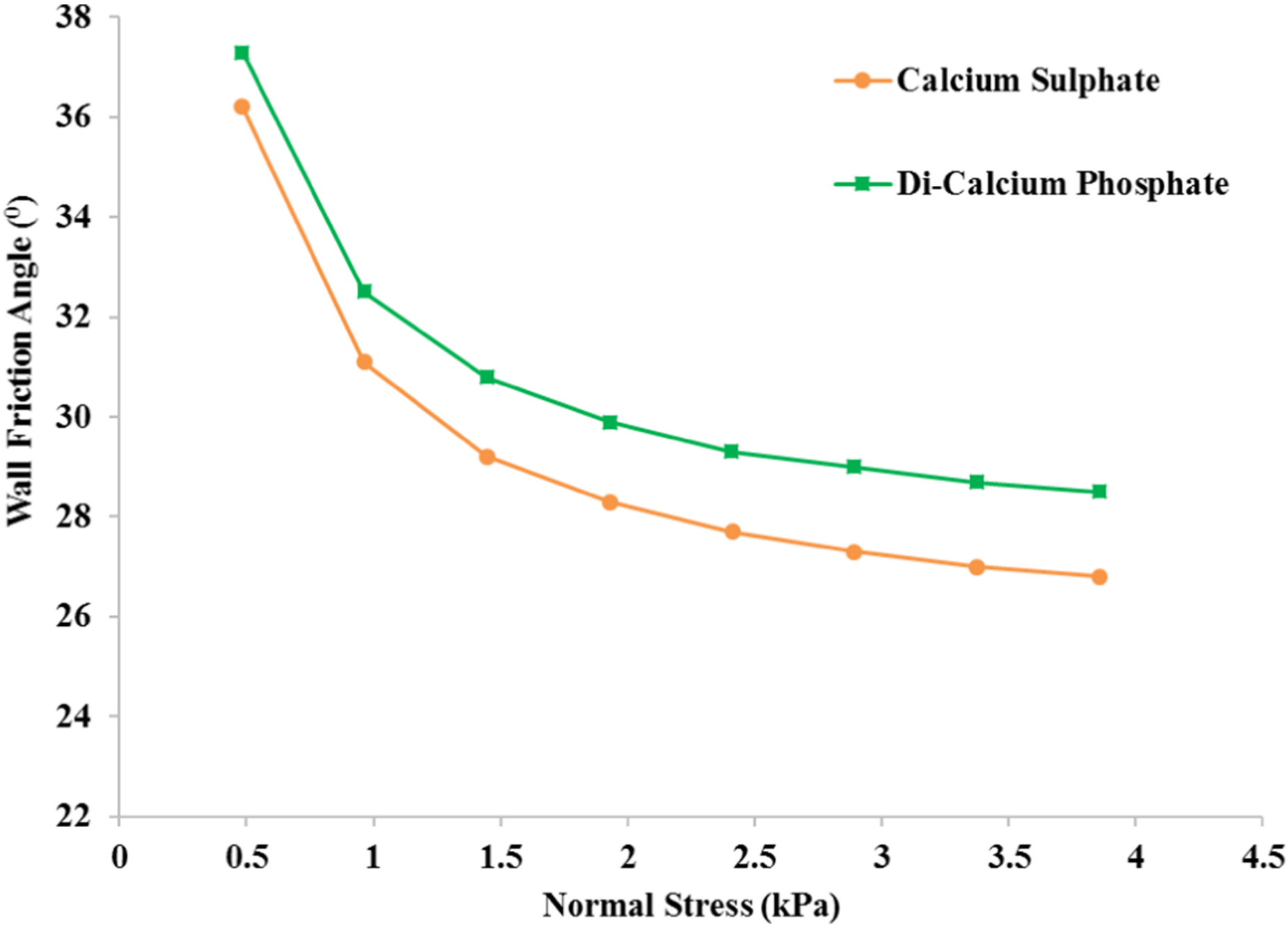
Calcium Sulphate
Di-Calcium Phosphate
Wall Friction Angle (°)
38
36
34
32
30
28
26
24
22
0
0.5
1
1.5
2
2.5
3
3.5
4
4.5
Normal Stress (kPa)

Figure 5

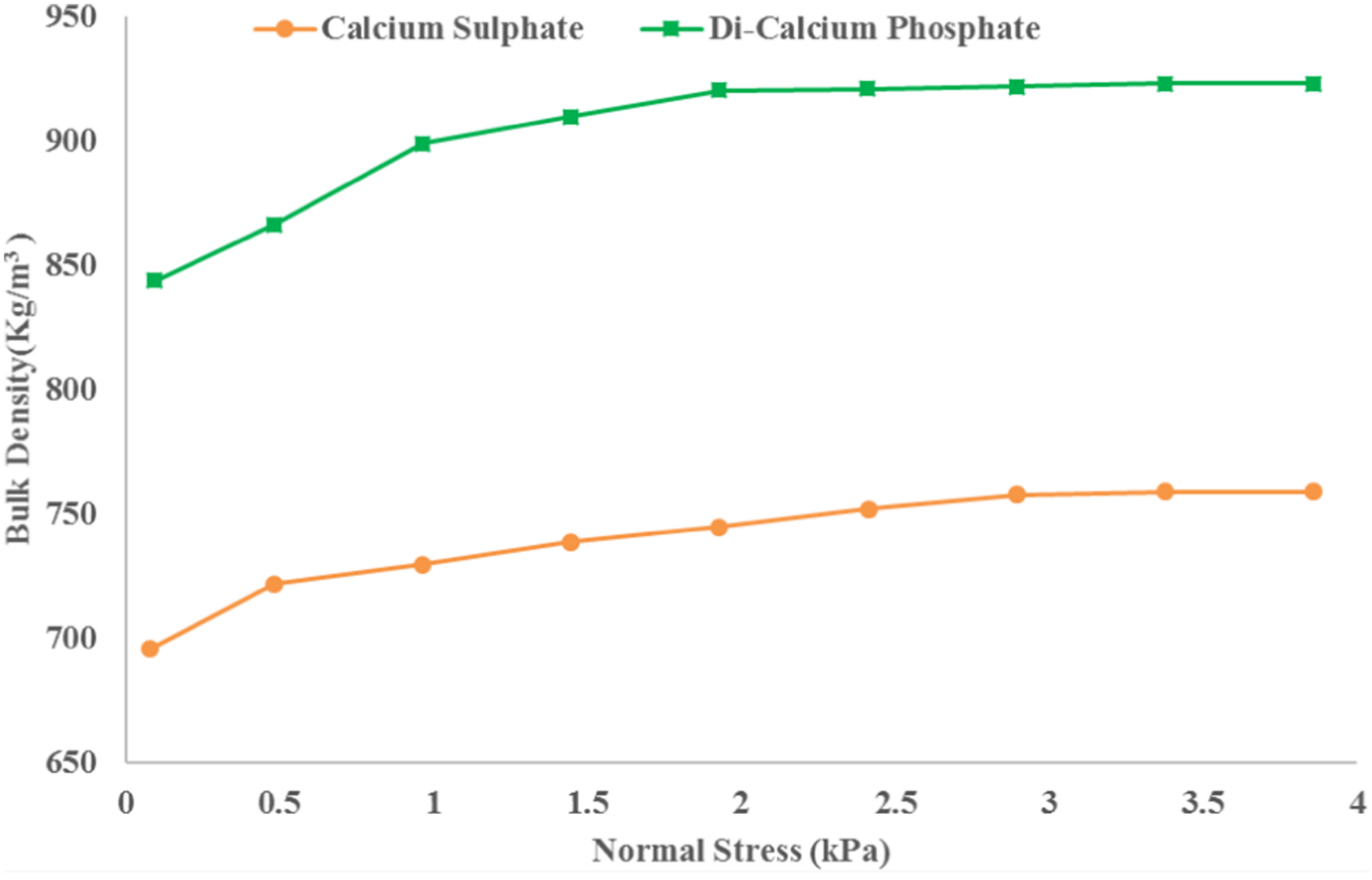
Calcium Sulphate
Di-Calcium Phosphate
Bulk Density(Kg/m³)
950
900
850
800
750
700
650
0
0.5
1
1.5
2
2.5
3
3.5
4
Normal Stress (kPa)

Figure 6

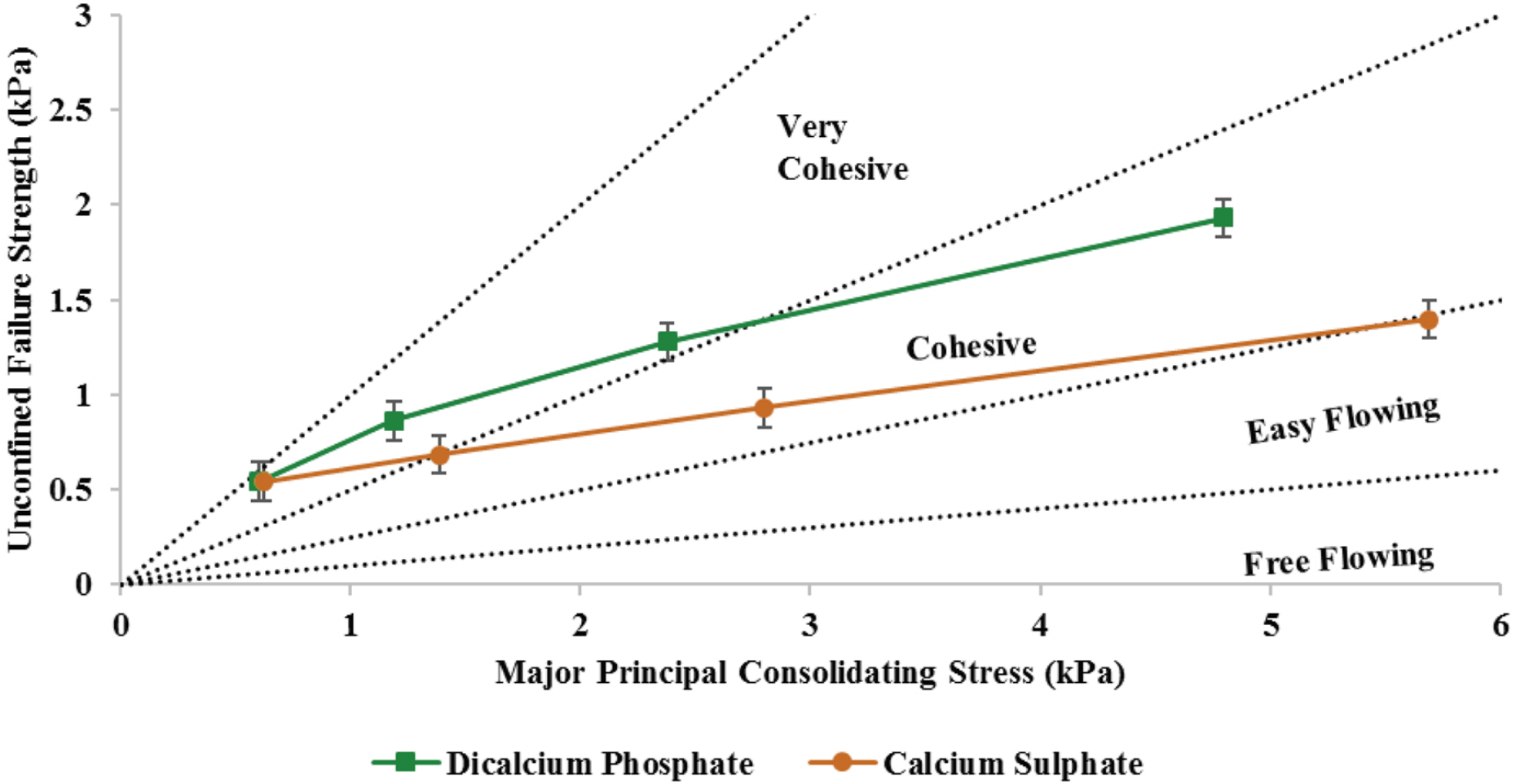
Unconfined Failure Strength (kPa)
3
2.5
2
1.5
1
0.5
0
0
1
2
3
4
5
6
Major Principal Consolidating Stress (kPa)
Very
Cohesive
Cohesive
Easy Flowing
Free Flowing
Dicalcium Phosphate
Calcium Sulphate

Figure 7

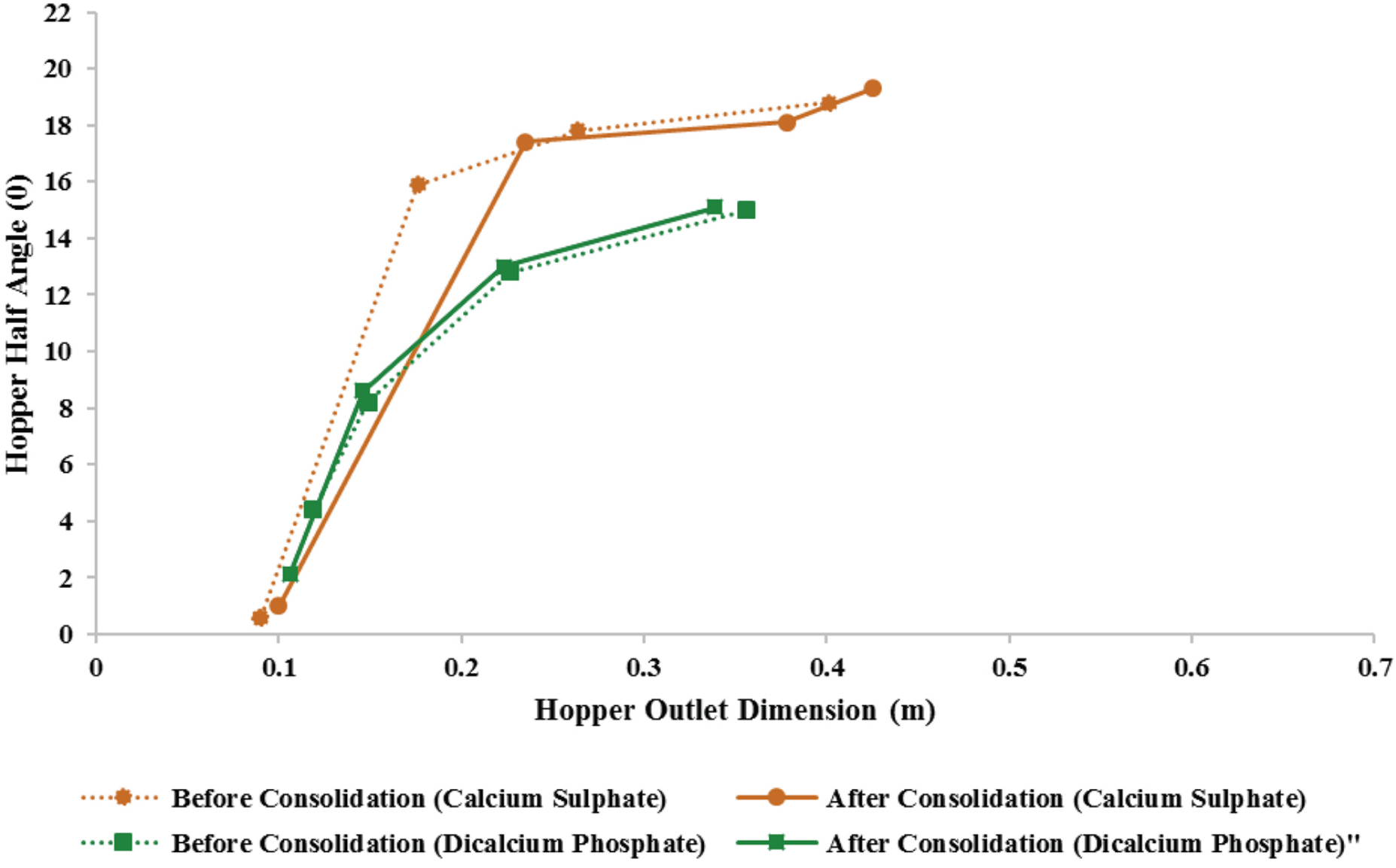
Hopper Half Angle (0)
22
20
18
16
14
12
10
8
6
4
2
0
0
0.1
0.2
0.3
0.4
0.5
0.6
0.7
Hopper Outlet Dimension (m)
Before Consolidation (Calcium Sulphate)
After Consolidation (Calcium Sulphate)
Before Consolidation (Dicalcium Phosphate)
After Consolidation (Dicalcium Phosphate)"

Figure 8

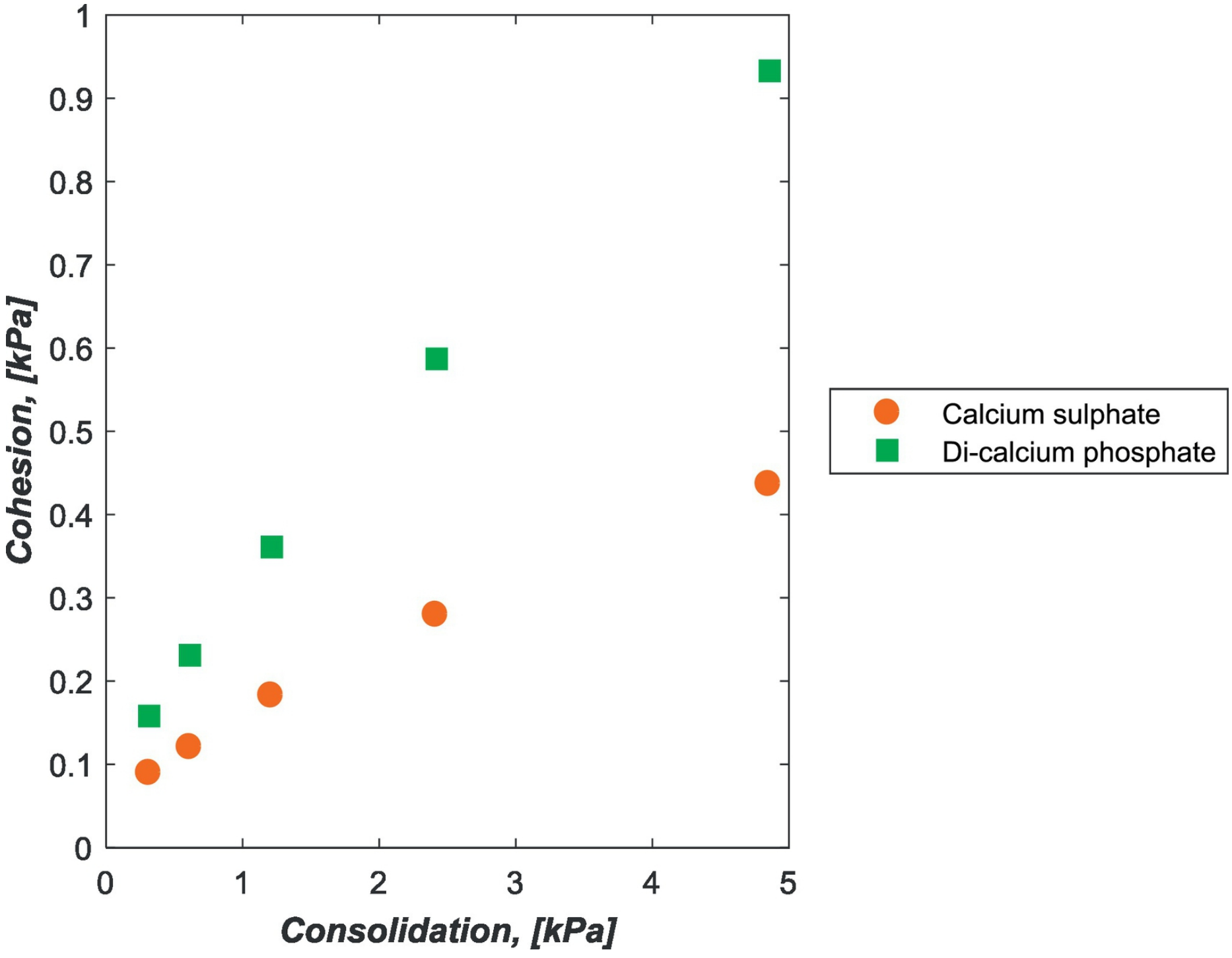
Cohesion, [kPa]
Consolidation, [kPa]
0
0.1
0.2
0.3
0.4
0.5
0.6
0.7
0.8
0.9
1
0
1
2
3
4
5
Calcium sulphate
Di-calcium phosphate

Figure 9

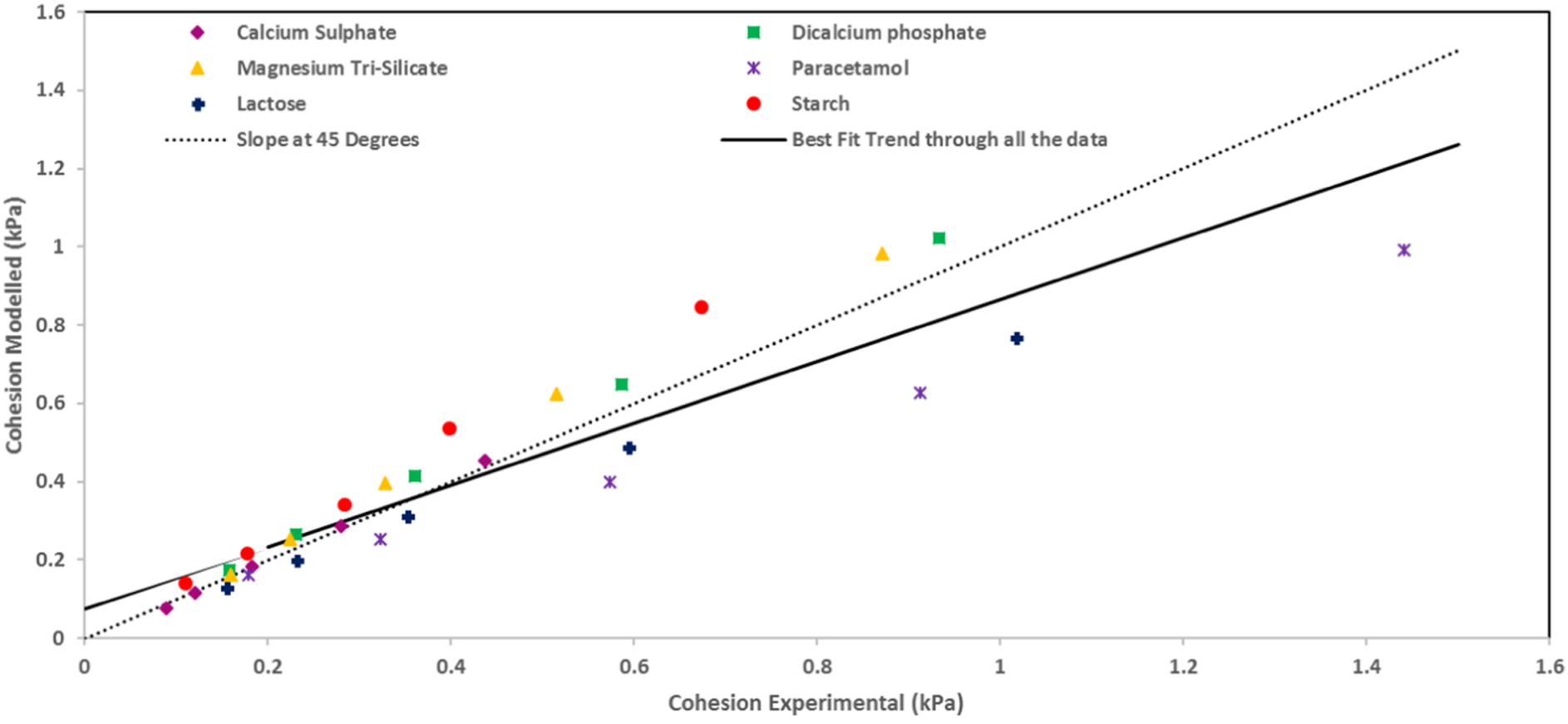
Calcium Sulphate
Dicalcium phosphate
Magnesium Tri-Silicate
Paracetamol
Lactose
Starch
Slope at 45 Degrees
Best Fit Trend through all the data
Cohesion Modelled (kPa)
Cohesion Experimental (kPa)
0
0.2
0.4
0.6
0.8
1
1.2
1.4
1.6

Figure 10

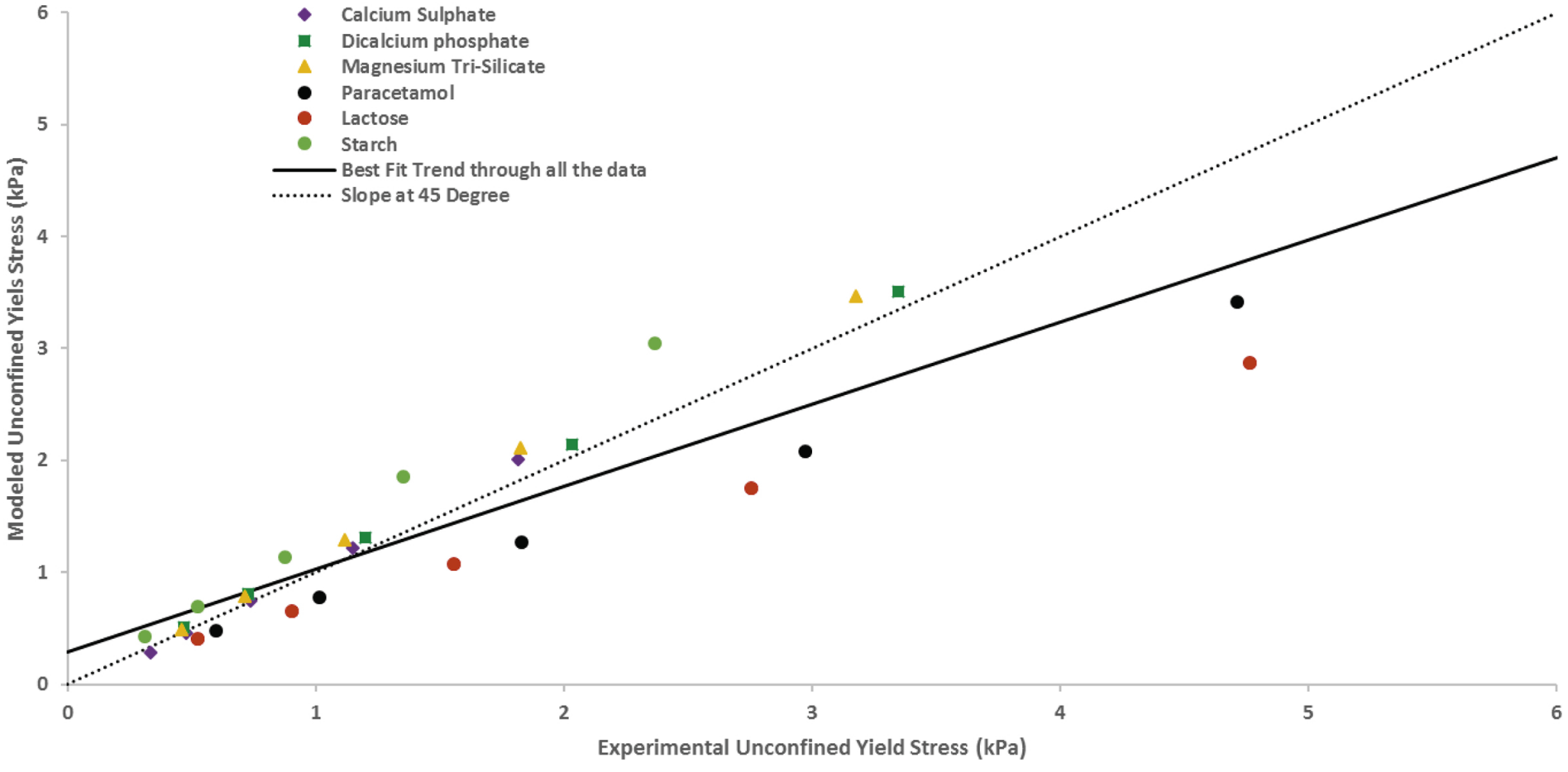
Calcium Sulphate
Dicalcium phosphate
Magnesium Tri-Silicate
Paracetamol
Lactose
Starch
Best Fit Trend through all the data
Slope at 45 Degree
Modeled Unconfined Yiels Stress (kPa)
Experimental Unconfined Yield Stress (kPa)
0
1
2
3
4
5
6

Figure 11